

8-2022

Induced Cytotoxicity In Crebbp/Ep300Mut Head And Neck Squamous Cell Carcinoma

Thomaia Pamplin

Follow this and additional works at: https://digitalcommons.library.tmc.edu/utgsbs_dissertations



Part of the [Genetic Phenomena Commons](#), [Genetic Structures Commons](#), [Medical Pharmacology Commons](#), and the [Other Medical Sciences Commons](#)

Recommended Citation

Pamplin, Thomaia, "Induced Cytotoxicity In Crebbp/Ep300Mut Head And Neck Squamous Cell Carcinoma" (2022). *Dissertations and Theses (Open Access)*. 1222.
https://digitalcommons.library.tmc.edu/utgsbs_dissertations/1222

This Thesis (MS) is brought to you for free and open access by the MD Anderson UTHealth Houston Graduate School at DigitalCommons@TMC. It has been accepted for inclusion in Dissertations and Theses (Open Access) by an authorized administrator of DigitalCommons@TMC. For more information, please contact digcommons@library.tmc.edu.

INDUCED CYTOTOXICITY IN *CREBBP/EP300*mut HEAD AND NECK SQUAMOUS
CELL CARCINOMA

by

Thomaia Pamplin B.A.

APPROVED:

APPROVED

Curtis Pickering, Ph.D.
Advisory Professor



Faye Johnson, M.D./Ph.D.

APPROVED

Heath Skinner, M.D./Ph.D.

APPROVED

Danielle Garsin, Ph.D.

APPROVED

Kunal Rai, Ph.D.

APPROVED:

Dean, The University of Texas
MD Anderson Cancer Center UTHealth Graduate School of Biomedical Sciences

**INDUCED CYOTOXICTY IN *CREBBP/EP300*^{mut} HEAD AND NECK
SQUAMOUS CELL CARCINOMA**

A
THESIS

Presented to the Faculty of

The University of Texas

MD Anderson Cancer Center UTHHealth

Graduate School of Biomedical Sciences

In Partial Fulfillment of the Requirements for the Degree of

Master of Science

In Biomedical Sciences and Cancer Biology

By

THOMAIA PAMPLIN, B.A.

Houston, Texas

August 2022

Dedication:

To John and Cora Pamplin, who poured their all into me.

To knowledge and community, that allows us to rise.

Acknowledgements:

First, I give all glory to God, the author and the finisher of my faith.

I want to thank my parents who have given me the ultimate support throughout my life in this pursuit of knowledge. I'm so grateful that I've enjoyed this ride overall. I know they'd support me on almost any path, but I will always be grateful that they prioritized education for me and my sisters.

I'd like to thank Dr. Curtis Pickering for taking this liberal Arts, English literature undergraduate student on board. He is one of the brightest people I have met. I learn something new every time I speak with him. The support that I've had from his lab was especially important during the socially tumultuous time of the COVID-19 pandemic.

I would also like to thank my committee members: Dr. Heath Skinner, who served as a co-mentor throughout my time. I appreciate your humor and optimism. Drs. Faye Johnson, Kunal Rai, and Danielle Garsin, thank you for sharpening me as a scientist.

Thank you to the Department of Head and Neck Surgery at MD Anderson, chaired by Dr. Jeffrey Myers. I have found friends and comrades in the fight to end cancer. Especially, Barbara DeLeon, Kelli Brown, Mason Bartels, Ayo Adebayo, Brandon, Charles Osamor, Dr. Nikhil Chari, Dr. Yoko Takahashi, Mei Zhao, Bing Bing, Dr. Abdullah Osman, and Dr. Burak Uzunparmak: bonding with you all made the days go by more enjoyably at times.

Lastly, I'd like to thank my friends who are like family and family who are like friends whose support outside of lab rejuvenated me within the lab. Thank you to Nicole, Ashley, Chalise, Ollisha, Danielle, Bri, Brandon Valyan, Daion Larmond, the Word of Life Ministry, the Clarkson/Jackson family, the Pamplin family and many others. I love you all.

Abstract:

**INDUCED CYOTOXICITY IN *CREBBP/EP300*mut HEAD AND NECK
SQUAMOUS CELL CARCINOMA**

Thomaia Pamplin

Advisor: Curtis Pickering, Ph.D.

Background: Head and neck squamous cell carcinoma HNSCC is the most common malignancy in the head and neck. Most cases are found in advanced stages and depending on the location can be treated with surgical resection and/or radiation (XRT), chemotherapy, or chemoradiation. Our lab groups have identified that HNSCC with a mutation in its *CREBBP/EP300* genes can be sensitized to XRT when the histone acetyltransferase activity of *CREBBP/EP300* is inhibited. This radiosensitization manifests in the form of increased cell death for *CREBBP/EP300*mut HNSCC treated with XRT. This project looks at the effect of two chemotherapeutic agents: cisplatin (CDDP) and doxorubicin (DOX) and the response that *CREBBP*mut HNSCC has to them when combined with a HAT inhibiting (HATi) drug called A485. We hypothesize that when combined with A485, *CREBBP*mut cells will undergo an induced apoptotic death when treated with DOX, and not cisplatin, because DOX induces DNA damage similar to that of XRT, in that homologous recombination is needed to repair the damage done by DOX.

Methods: *CREBBP*-mut HNSCC cell lines UMSCC-22A and UMSCC-17B and *CREBBP*-wt HNSCC lines HN31 and FADU were used in cell culture. Clonogenic survival assays were used to cell growth and death with the different agents (DOX, CDDP, XRT with or without A485) used in single and combination treatments. Flow cytometry was used to

measure cell death and apoptosis. Cell Titer Glo was used to measure cell viability after using the three different agents in alone or in combination with A485. Western Blot was used to determine if apoptosis occurred with these treatments in the four cell lines by probing for cleaved caspase 3 and PARP products.

Results: Using clonogenic survival assays to observe cell growth on inhibition of growth, a consistent and conclusive of an enhancement of cell death with cisplatin+A485 combination for CREBBPmut and wt HNSCC cells was not observed. Using real-time quantitative live-cell imaging and analysis platforms through an Incucyte, cell death was measured.

Significant differences in cell death between CREBBPmut and wt cell lines treated with DOX+A485 was not observed. Western Blot analysis also did not lead to consistent apoptosis cleavage products in CREBBPmut HNSCC cell lines when treated with DOX, XRT, or CDDP alone or in combination with A485.

Conclusion: An enhancement of cell death with DOX+A485 was not observed, nor was apoptosis consistently observed in the cell death response for CREBBPmut HNSCC cell lines treated with DOX alone in or in combination with A485; therefore, the hypothesis was not proven to be true. Some of the experiments performed in this project have been reproducible in the hands of others, so perhaps with more time and support in trouble shooting, our group may be able to reproduce the XRT results seen in previous findings and more trustworthily determine if DOX leads to a similar phenotype. This project has the potential to help characterize the mode of cell death and DNA damage that occurs in induced cytotoxic response which could eventually help with patient outcomes and quality of life, as chemotherapy and XRT come with many toxicities.

Table of Contents

Thesis Approval.....	i
Title Page.....	ii
Dedication	iii
Acknowledgements	iv
Abstract	v
Table of Contents	vii
List of illustrations.....	viii
List of Tables.....	viii
Chapter 1: Background.....	1
Chapter 2: Materials and Methods	10
Chapter 3: Results	14
Chapter 4: Discussion.....	31
References.....	37
VITA.....	44

List of Illustrations

Figure 1..... 17

Figure 2..... 18

Figure 3..... 19

Figure 4..... 21

Figure 5..... 22

Figure 6..... 24

Figure 7..... 25

Figure 8..... 26

Figure 9..... 27

Figure 10..... 29

List of Tables

Table 1..... 31

Chapter 1: Background

Head and neck squamous cell carcinoma (HNSCC) usually develop in the mucosal epithelium of the oral cavity, pharynx, and larynx and is the most common malignancy in the head and neck. Its occurrence generally correlates with exposure to tobacco-derived carcinogens, excessive alcohol consumption or both. HNSCC can also be linked to oncogenic strains of the human papillomavirus (HPV), mostly HPV-16, and less frequently, other strains. HPV is the major factor in oropharynx cases while tobacco and/or alcohol are the primary factors for oral cavity and larynx sites.

Though the first vaccine to help prevent HPV was approved by the FDA in 2006, the effects of vaccination will take decades to be fully known.¹ In 2021, there were approximately 54,000 new cases and 11,230 deaths from oral cavity or oropharyngeal cancer.² Detection of HNSCC occurs through physical examination since there are no screening strategies for the disease. There are pre-malignant lesions that may form in the mouth such as leukoplakia or erythroplakia, white and red patches respectively. However, most cases are found in the cancer's advanced stages. Oral cavity and oropharyngeal cancers occur mostly in the oropharynx which consists of the tongue, tonsils, gums, the floor and other parts of the mouth.² For oral cavity cancer, especially early-stage tumors, the general treatment standard is surgery with or without adjuvant XRT. Radiotherapy for locally advanced oropharyngeal cancers leads to significantly less severe or fatal complications compared to surgery.^{2,3} For early-stage oropharyngeal disease, a single modality, historically XRT, is preferred. However, new surgical options such as transoral robotic surgery are

becoming increasingly common. Locally advanced oropharynx tumors induced by HPV respond better to radio-chemotherapy than those induced by tobacco and alcohol.

Cancers that begin in the larynx, also known as the voice box, are called laryngeal cancers and hypopharynx cancers start in the lower throat.⁴ This cancer is usually treated with XRT or chemoradiotherapy since it is more likely to preserve larynx function when compared to surgical excision.⁵ Most cases of HNSCC require a multimodal approach. The staging and treatment selection are chosen based on the initial site of the tumor and then include the other factors mentioned above. Additionally, studies have shown that patients with HPV+ head and neck cancer have significantly improved survival outcome compared to patients with HPV- cancer.⁶ This finding has led to a clinical push to de-intensify therapy by reducing XRT and/or chemotherapy dosage.

Tumor staging and sizing is done to determine whether a surgical procedure is needed and what type. Surgical margins (SM) and metastatic lymph nodes are the major determinants of choosing to use post-operative XRT.⁷ Perineural invasion (PNI) and extracapsular spread (ECS) are also two important factors in treatment planning. PNI is the spread of neoplastic cells from their original site into the space between or beneath the perineurium layer.⁸ The occurrence of ECS is associated with increased regional recurrences, and nodal and distant metastases in head and neck subsites, including the larynx and oral cavity⁹. Positive SM or ECS are usually treated with the addition of cisplatin-based chemoradiotherapy to XRT. ECS of metastatic HNSCC to regional lymph nodes is the most reliable indicator of poor treatment outcomes.¹⁰

Cisplatin-based chemoradiotherapy is deemed to be the first-line treatment for patients with locally advanced HNSCC (following surgery for some tissue sites). Although

another drug, cetuximab, an FDA approved-EGFR-targeting monoclonal antibody, has increased survival and loco-regional control with combination treatment of cetuximab and XRT compared to only cetuximab alone in one study.¹¹ However, another study comparing cetuximab, and cisplatin (CDDP) in combination with XRT, there was not a significant difference between the two treatments with long-term use.¹² The varying results of therapies that may provide better patient outcomes presents a need to find treatments that could provide better survival outcomes and quality of life for HNSCC patients.

There are multiple types of chemotherapeutic agents including alkylating agents, antimetabolites, anti-microtubule drugs, topoisomerase inhibitors, and antitumor/cytotoxic antibiotics. Cisplatin (CDDP) a metal salt belonging to the alkylating agent family and doxorubicin is an antitumor antibiotic, specifically an anthracycline. Alkylating agents can add alkyl groups to proteins, RNA and DNA. Binding alkyl groups to DNA can cause intrastrand or interstrand crosslinks that can cause the DNA strands to break during DNA replication and lead to apoptosis.¹³ This project looks at the effect of CDDP or doxorubicin in combination with a histone acetyltransferase (HAT) inhibiting drug, A485. Cis-diamminedichloroplatinum, or more commonly known as CDDP, was the first heavy metal compound discovered to have antineoplastic activity and has gone through much clinical and preclinical investigation since 1965. CDDP appears to directly bind with DNA to bring about its cytotoxic effects due to the ‘cis’ position of its chloride and ammonia group which allows rapid DNA binding. The cis-isomer of this drug cross links between guanine-guanine groups on DNA. CDDP directly impairs non-homologous end-joining (NHEJ) independent of downstream DNA damage responses.¹⁴ CDDP is synergistic with XRT and other chemotherapeutic agents. In patients, CDDP is usually administered intravenously every 3-4

weeks with a dose range between 50-120 mg/m² of a body surface area as a single dose or divided over 5 days.¹⁵ Recently, there has been increased interest in using 40 mg/m² weekly which has similar efficacy with less toxicity.¹⁶ Many studies are now switching to this regimen.

Anthracyclines, a type of cytotoxic antibiotic, can kill cells through DNA intercalation, topoisomerase II poison, generating excessive reactive oxygen species, and DNA adduct formation. Studies have shown that their antitumor activity stems from their ability to insert themselves into the DNA helix and/or covalently bind to DNA replication and transcription proteins. Doxorubicin intercalates base pairs of DNA's double helix by binding to targets such as topoisomerase I and II. Topoisomerases assist in DNA repair in multiples ways such as making reversible cuts in DNA at sites with too much tension or where DNA replication occurs. then these sites get repaired during DNA replication. When doxorubicin binds topoisomerase, it ceases DNA replication and ultimately RNA transcription.¹⁷ These interactions inhibit the synthesis of DNA, RNA, and proteins, which leads to cell death.¹⁸

DNA damage induced by doxorubicin is repaired primarily by the homologous recombination (HR) repair pathway.¹⁹ Doxorubicin (DOX) was isolated from *Streptomyces peucetius* in the 1960s. It is one of the most powerful antineoplastic agents. It is used as a solid tumor and hematological treatment.

Clinically, DOX is not a therapy used in patients with HNSCC. I studied DOX effects because of its mechanism of action rather than its translatability to the clinic. There are few studies that have been done with HNSCC cell lines and doxorubicin, specifically looking at drug delivery. For example, a study on nanodelivery saw that when doxorubicin is co-

delivered with a HIF-1 inhibitor drug, the uptake of doxorubicin was enhanced and improved efficacy in oral squamous cell carcinoma.²⁰ Another group used DOX and hydrogels and discovered a new drug delivery system with intratumoral injection that could be a promising chemophoto-therapy alternative for HNSCC.²¹

My hypothesis is that DOX induces the homologous repair pathway which leads to an induced cytotoxic response in *CREBBP/EP300*mut HNSCC. Therefore, distinguishing between NHEJ and HR. NHEJ is a DNA damage repair pathway that fixes double stranded breaks. In this pathway, DNA is repaired directly, without needing a homologous strand of DNA to use as a template.²² Regions of microhomology, which are the degradation of 5' and 3' overhangs, direct the strands for end joining.²³ The strands undergo a strand invasion, DNA synthesis and resolution, then they are ligated together by DNA ligase IV and X-ray repair cross-complementing protein 4 (XRCC4).

HR is also a repair pathway for double stranded DNA breaks. This type of repair is template dependent. HR also duplicates the genome by supporting gDNA replication and telomere maintenance, thus having an important role in genome preservation. HR can be divided into three phases: presynapsis, synapsis, and postsynapsis. In presynapsis the overhanging strands of DNA are recognized. In synapsis, strand invasion where the single-stranded DNA moves into another DNA duplex. Post synapsis may involve multiple rounds of invasion and synapsis that leads to final product of repaired double stranded DNA.²⁴

Additionally, our group performed in vivo shRNA library screens in irradiated tumors made from five HNSCC cell lines with different HPV status and genetic backgrounds. They used two libraries: one which contained genes that were targetable for antineoplastic agents currently used in clinic and another that targeted DNA damage repair pathways. They

identified several targets such as CDK6, XIAP, and PIK3CA that were associated with radiosensitization and they identified DNA-damage repair genes such as TP53, BP1.²⁵ They then determined that somatic mutations in *CREBBP/EP300* genes in HNSCC were associated with these radiosensitizing targets by comparing the redundant shRNA log p-values they obtained in the library screens and the median fold change data for radiosensitizing targets between mutant and wildtype HNSCC cell lines. From this analysis, they saw that several targets were increased in NOTCH1 and CREBBP mutant tumors. After identifying these targets in HNSCC, our groups have found that there is increased radiosensitization in *CREBBP/EP300* mutant HNSCC cell lines when the corresponding gene is inhibited by shRNA (knock-down or KD).

CREB-binding protein and p300 are highly conserved transcriptional coactivators with approximately 75% overall sequence identity and greater than 90% sequence identity in their HAT domains.²⁶ The gene products of *CREBBP/EP300* are the CREB-binding protein (CBP) and p300; and they can have distinct roles in certain contexts, but many of their functions are redundant, so they are commonly referred together as CBP/p300. One major function for CBP/p300 is modulating basal transcription through chromatin remodeling and recruiting transcription factors and activators.²⁸ CBP/p300 has intrinsic HAT activity and can relax chromatin. CBP/p300 can also acetylate transcription factors and regulate their activity.²⁹

CBP/p300 modulate transcription and stabilizes itself at the promoter regions on genes through multivalent interactions between tandem transactivation domains (TADs) and intrinsically disordered regions (IDRs). Structurally, CBP/p300 can also act as a bridge between DNA binding and general transcription factors, linking activators to basal

transcription machinery through interactions with transcription factor II-D (TFIID), which is made of the TATA-binding protein (TBP): TBP-associated factors (TAFs) general transcription factor. TFIIB, and RNA polymerase II. CBP/p300 has a critical role in forming the preinitiation and reinitiation complexes that facilitate multiple rounds of transcription.³⁰

Overall, CBP/p300 has been found to engage in hundreds of different transcriptional factors' activities, the proteins can also be regulated by phosphorylation. Studies have shown that cell-cycle dependent phosphorylation occurs on p300 by cyclin E/Cdk2. Additionally, CBP/p300 have a protein kinase A (PKA) site and several studies have proposed that phosphorylation of CBP/p300 by PKA regulate the two proteins. CBP can also recruit itself to induce transcriptional activation and is known to recruit other HATs such as P/CAF, p/CIP, and SRC-1.

Findings that STAT-2 and the p65 subunit of NF-kB compete for the same site on CBP/p300 but are not mutually antagonistic for the CBP/p300 first zinc finger domain suggest that CBP/p300 are at a limiting concentration in the cell. Three important and drug targetable domains on CBP/p300 include its bromodomains, HAT domains, and TADs.

CBP/p300 can remodel chromatin by acetylating histone H3.³¹ It relaxes chromatin with its HAT activity at the gene's promoter.³² CBP/p300 have been found to facilitate double stranded break (DSB) repair on DNA by acetylating histones H3 and H4 on chromatin DSB sites.³³ CBP/p300's HAT activities have shown to regulate DSB repair by acetylating histones at promoter regions of HR-related genes and acetylating histones at DSB sites which also activates recruitment for HR repair proteins.³⁴ BRCA1, a gene with many functions in DNA repair, and RAD51, a gene that specifically function in HR have been shown to be transcriptionally regulated by CBP/p300.

Additionally, our groups examined apoptosis via TUNEL staining for HNSCC treated with XRT and a *CREBBP* KD and observed significantly increased staining in *CREBBP*mut cell lines but not wild type. They also observed through immunoblot assays that *CREBBP* KD in combination with XRT lead to cleaved caspase 3 products, an indicator that apoptosis is active. Via immunofluorescence staining of DNA-damage foci, our group looked at the DNA-damage response within this radiosensitive phenotype. They found that DNA damage marker, γ -H2AX foci, was increased after *CREBBP* KD and XRT in three *CREBBP* mutant cell lines and one *EP300* mutant cell line. The effects of knocking down *CREBBP* and treating tumors with XRT was also investigated by using three different in vivo models of HNSCC, two with mutant *CREBBP* and one harboring wildtype *CREBBP*. This study showed that with *CREBBP* KDs and XRT there is significant tumor-growth delay, improved survival, and decreased tumor volume in mice models injected with *CREBBP* mutant cell lines compared to mice injected with *CREBBP* wt cell lines.²⁵

Our groups also used chemical inhibitors of CBP/p300 function to study the therapeutic relevance of the radio sensitizing phenotype. They used ICG-001, a CBP-specific inhibitor, GNE-272, a bromodomain inhibitor, and A-485, a HAT inhibitor specific for CBP/p300 and found that A-485 led to profound radiosensitization in *CREBBP* or *EP300* mutant cell lines. They then examined the relationship between HAT inhibition and HR using an I-SceI-based assay and found that A-485 resulted in a significant repression of HR in *CREBBP* or *EP300* mutant HNSCC cell lines and had little effect on NHEJ in HNSCC cell lines.²⁵

My project aims to determine if doxorubicin, which affects the HR pathway, will lead to an increase cytotoxic response compared to a single treatment condition without A485,

such as the one seen with XRT in our group's previous findings. I compared the effect of doxorubicin in combination with HAT inhibition by A485, with a combination treatment with CDDP and A485. As CDDP affects the NHEJ repair pathway, we hypothesize that the same induced cytotoxic response seen with XRT and HATi will not occur with CDDP. I also examined if doxorubicin or CDDP in combination with A485 leads to an apoptotic death as seen in previous findings with XRT. We predict that *CREBBP*mut HNSCC cells undergo apoptosis following combination with HAT inhibition and XRT due to a dysfunction in the HR repair pathway. I will test this hypothesis by using DOX which affects HR, CDDP which affects NHEJ, and observing the cell death and DNA damage that occurs with these treatments.

Chapter 2: Materials and Methods

Cell Culture: HNSCC cell lines, UMSCC-22A, UMSCC-17B, HN31, and FaDU were obtained from the Myers laboratory.²⁴ Each cell line was sustained in Dulbecco modified Eagle medium, nutrient mixture F-12, high glucose, with L-glutamine and sodium bicarbonate, without HEPES. This media was supplemented with 10% FBS and 1% penicillin/streptomycin. Each cell line was incubated at 5% CO₂ atmosphere and 37° Celsius.

A-485 and A-486 were made at the MD Anderson Institute for Applied Cancer Science or purchased from Selleckchem (#S8740). Doxorubicin (Adriamycin) HCl is from Selleckchem (#S1208). CDDP was provided by the MD Anderson Pharmacy, from Accord (McKesson #NDC1672928838).

The irradiator used in these experiments is Mark I-68.

Clonogenic Survival Assay: 500-4000 cells were plated in low densities from the cell lines mentioned above in 6-well plates. Cells were plated on day 9, treated with A485/A485 on Day 1, treated with XRT, DOX, or CDDP on Day 3, 24 hours after the A485/A486 treatment. This treatment timeline was used for flow cytometry, Western blot, and Incucyte analyses. The cells were monitored during an incubation time of 7-14 days. Plates were collected when the cells formed colonies containing 50-100 cells. Subsequently, the plates were fixed and stained with 0.25% crystal violet/methanol solution, then scanned and analyzed through ImageJ software where colonies consisting of 50 colonies and more were counted. GraphPad prism (v9.0) was used to create survival curves of the ImageJ analysis outputs.

Flow Cytometry: Cells were plated into 6-cm dishes and given 24- and 48-hour treatments of XRT, DOX, or CDDP with or without A485 and puromycin as a positive control. Floating dead cells and trypsinized cells were washed in Corning 1X Phosphate-buffered salt (PBS) solution that did not contain calcium or magnesium and collected in round bottom tubes. After being spun in a centrifuge for 5 minutes at 1000rpm, cell pellets were obtained, and the supernatant was vacuumed out of each sample. The samples were then placed on ice and the pellets were resuspended in 50uL of 1X Annexin V buffer (BD Biosciences). 2uL of a 1:2.5 dilution solution of Sytox Blue Dead cell stain (Thermo Fisher #S34857) in 1X Annexin V buffer was added to the sample, along with 2uL of Annexin V-APC (Thermo Fisher #A35110). The samples' tubes were flicked to mix, covered with aluminum and stored in the dark for 30 minutes. After thirty minutes, 250uL of 1X Annexin V binding buffer was added and the samples were analyzed for flow cytometry.

The samples were analyzed in a Beckman Coulter Gallios 561 flow cytometer at MD Anderson Cancer Center North Campus Flow Cytometry and Cellular Imaging Facility. Preliminary results were gathered from this core facility and further results were analyzed using FlowJo (v10.8.1).

Incucyte: Single cells were plate 96 well dishes and placed in an Incucyte S3 Live-Cell Analysis instrument (Sartorius #4647). 1:4000 (250nM) dilution Cytotox green dye (Sartorius #4632) was used to count dead cells. Images were taken by the Incucyte at 10X magnification every 4-6 hours for 72 hours.

Through the Incucyte programming phase object confluency and fluorescing green object count were measured. Image analysis training was applied to each experiment to accurately measure confluency and green object count. Measurements were exported to excel, and

curves and plots were developed in GraphPad prism by normalizing the green count object to phase object confluency (v9.0).

The plate is placed in an incubator with 5.0% CO₂ atmosphere and 37 degrees Celsius throughout the live cell imaging and analysis.

Cell Titer Glo: Following Incucyte experimentation, the plates were taken out of the Incucyte and equilibrated for 30 minutes in room temperature. Subsequently, CellTiter-Glo Viability Assay reagent (Promega #G7572) was added to the wells in equal volume to the solution that already existed in the wells. The plates were then orbitally shaken for 2 minutes and then transferred to a 96-well solid white-bottomed plate. Afterwards, the samples were allowed minutes to stabilize the luminescent signal. The luminescence of each well was then analyzed in the FLUOstar Omega (BMG LABTECH INSERT Software v. 3.00 R3, firmware v.1.32)].

The outputs from the FLUOstar Omega were analyzed in GraphPad prism (v9.0) to create plots.

Western Blot: Cells were plated in 10-cm dishes and treated with DOX, XRT, or CDDP with or without A485 over the course of 48 hours. Cells were trypsinized and collected at 72 hours. Cells were placed in a 1X RIPA lysis buffer (Millipore #20-188) that contained 1X protease inhibitor, 10mM NaF, 1mM Na₃VO₄, 10mM NaPP, and 1mM PMSF.

Obtaining the protein concentration of these samples was done by adding serial dilutions of 4ug/mL stock concentration of BSA in triplicate to a 96-well plate and adding the samples in triplicate to the same plate. The plate was then measured in a FLUOstar Omega (BMG LABTECH Software v. 3.00 R3, firmware v.1.32) where absorbance was measured at

570nm. Protein sample containing 160ug of protein were created using 5X loading dye and lysis buffer.

Cells were loaded into Mini-PROTEAN TGX gels (Bio-Rad #4561094, #4561096), placed into gel electrophoresis chambers, and those chambers were filled with 1X running buffer. The gels ran for 30 minutes at 80 volts, and then 100-120 volts until the dye reached the bottom of the gels.

PVDF membranes were placed in methanol for 3 minutes, then immersed into 1X transfer buffer. From there, sponges were immersed in 1X transfer buffer, the gel was transferred from there to the membrane, then to more of the sponge and these were placed into the Trans-Blot Turbo (Bio-rad #1705140) and ran for the pre-programmed 2 gels for 10 minutes.

The membranes underwent standard Western blotting procedure of being washed in 1X TBS-T, blocked in 5% milk-TBS-T and probed with the primary antibodies cleaved caspase 3 (Cell Signaling #9661S), CASPASE 3 DETAILS, and PARP (Cell Signaling #9542S).

Secondary antibodies used were Goat Ant-Mouse IgG (H+L)-HRP Conjugate (BIO-RAD #1706516) and Goat Anti-Rabbit IgG (H+L)-HRP Conjugate (BIO-RAD #1721019).

Chapter 3: Results

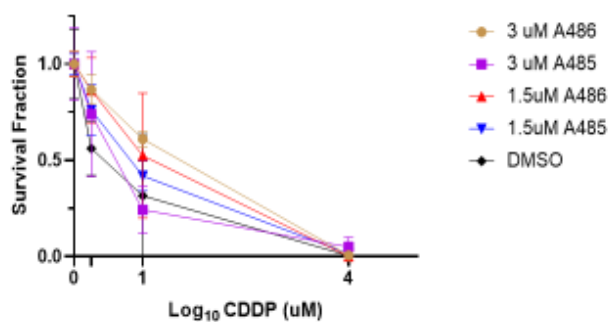
Increased cell death response was not observed consistently in clonogenic survival assays for *CREBBP*-mut HNSCC treated with XRT and HATi compared to *CREBBP*-mut HNSCC treated with CDDP + HATi

To investigate the survival outcomes of cells treated with 0-4 μ M CDDP, and 0-6Gy XRT, in combination or without 1.5 and 3 μ M A-485, clonogenic survival assays were conducted with *CREBBP/EP300*-wt cell lines HN31 and FADU, and *CREBBP*-mut cell lines UMSCC-17B and UMSCC-22A. These doses were chosen after performing plating efficiency experiments in which 50-8000 cells were plated in one well on a 6-well plate. Wells with higher densities received a higher dose and the IC₅₀ was determined. For CDDP, the IC₅₀ was 1 μ M and for XRT the IC₅₀ dose was between 2 and 4Gy. IC₅₀ was used so we could determine the dose at which an effect is observed with a single agent, but not so drastic of an effect, that we would not be able to see a potential enhancement of phenotype when the second agent, A485, was added. In patients the C_{max} for CDDP is 3200-3600 μ g/L or 11-12 μ M.²⁷ We hypothesized that there would be increased cell death when XRT and DOX were in combination with A485, but not with CDDP. UMSCC22A and UMSCC17B were treated with CDDP in combination with A485 or A486, an inactive version of A485 used as a vehicle control. No significant difference between were seen in these cell lines between cells treated with CDDP alone or in combination with A485 (Figure 1). Both UMSCC17B (*CREBBP* mutant) and FADU (*CREBBP*wt) had a significant difference at 6Gy between the no treatment condition and the 1.5 μ M and 3 μ M groups. At 0Gy, 2Gy, and 4Gy, there was no significant difference for either cell line when treated with A485 (Figure 2).

Clonogenic assays had inconclusive results because the cells ceased to grow into colonies or would grow at variable rates on the plates as we continued these experiments. Different incubators, media, and 6-well plates were tested but for months, inconsistent results were obtained from clonogenic survival assays. Figure 3 displays the inconsistent colony growth that frequently occurred in clonogenic experiments. The top wells have a lower density that led to no colony growth. The bottom wells of each plate had higher initial cell density. The rings that are seen in the wells that had some colony growth may be from the incubator vibrating. It is more difficult to determine why the outside wells have less cell growth.

Overall, the hypothesis that increased cell death would be observed in *CREBBP*-mutant cell lines when treated with XRT and HATi was not seen consistently or exclusively in clonogenic survival assays.

A. UMSCC22A (1200-cell/well) CDDP + HATi



B. UMSCC22A (2400-cell/well) CDDP + HATi

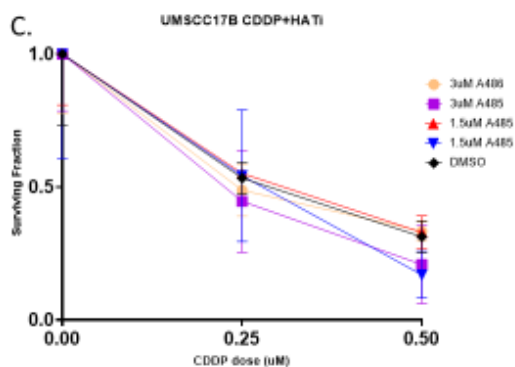
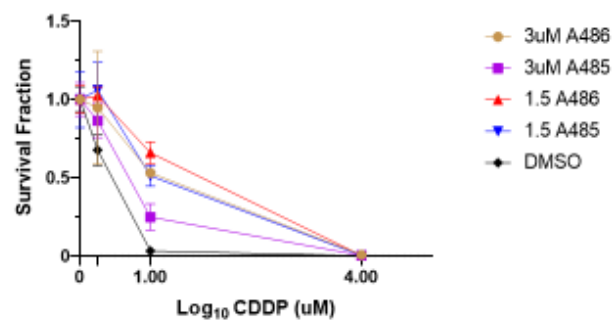


Figure 1: (A) UMSCC22A, CREBBPmut HNSCC, showed no significant differences between Cisplatin (CDDP) only treated groups and CDDP in combination with HAT inhibition (A485). (B) UMSCC22A, plated in initial higher densities than figure 1A showed no significant difference between CDDP only and CDDP in combination with HAT inhibition. (C) UMSCC17B showed no significant difference between CDDP only and CDDP in combination with HAT inhibition.

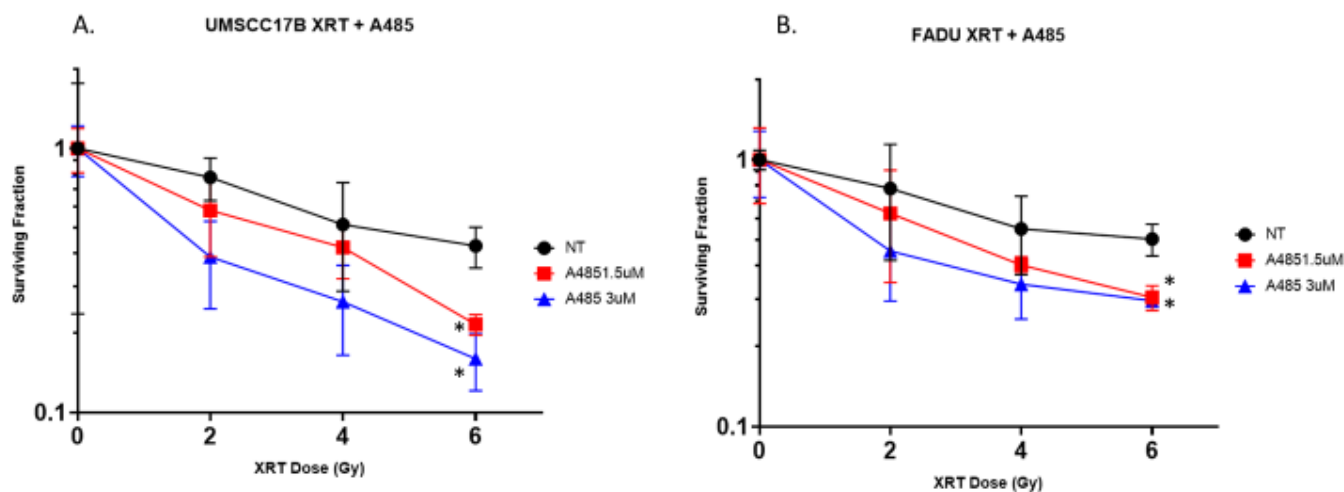


Figure 2: (A) No significant difference between conditions treated with radiation (XRT) at a 0, 2, and 4Gy dose alone or in combination with HAT-inhibition (A485) was measure in CREBBPmut cell line UMSCC-17B. (B) No significant difference was measured in CREBBPwt cell cline FADU, between cells treated with XRT at a 0, 2, and 4Gy dose alone or combination with HATi.

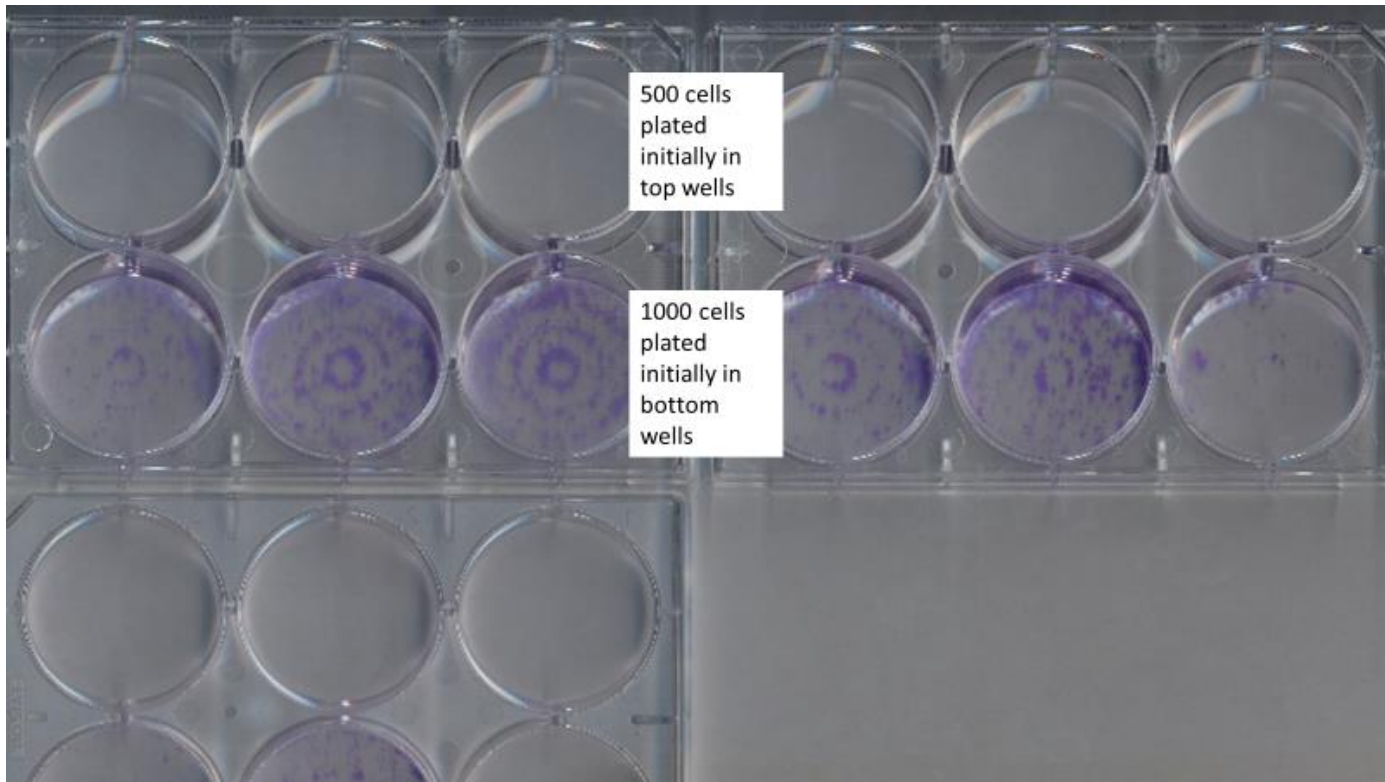


Figure 3: From top left clockwise, Denville, NEST, and Falcon 6-well plates. Unequal growth and rings are seen in the wells.

No apoptotic phenotype or increased cell death was observed in *CREBBP*^{mut} HNSCC treated with XRT or CDDP and A485 in flow cytometry assays

To have another measure of cell death and measure the amount of apoptosis occurring with these treatments, flow cytometry experiments were performed. The flow cytometry experiment would test my hypothesis by allowing a comparison between XRT only conditions and XRT in combination with HATi (A485). Using Annexin-V APC to stain early apoptotic cells and SytoxBlue, a non-permeable stain that would indicate a necrotic or late-stage apoptotic death, we did not observe a significant difference between the HNSCC cells treated with XRT alone or in combination with A485 HAT inhibition. We used this method because it provided an orthogonal measure of cell death to the clonogenic assays and Western blot experiments that probed for cleavage products of apoptotic proteins such as

caspase 3. We employed the same timeline and drug doses as seen in Figure 8 to measure cell death. In XRT experiments using both *CREBBP*^{mut} and *CREBBP*^{wt} HSNCC cell lines, we did not find a significant difference between conditions with XRT alone or in combination with HATi. This is not a finding that has been observed in previous studies and gives inconclusive results for our hypothesis. Figure 4 shows the results of flow cytometry measuring Annexin V-APC on the x axis and Sytox Blue on the y. Quadrant I represents live cells while Quadrant II and III contains cells positively stained with Annexin V-APC, thus positive for apoptosis. Quadrant III and IV represents cells stained with Sytox Blue that are in a late apoptotic or necrotic stage. There is not a significant difference between the XRT conditions alone and with A485 (Figure3). Additionally, there is not a significant difference between the treated groups and the non-treated groups which means we were not seeing a cell death response either. Figure 5 is a quantification of these results. The lack of cell death with these treatments prompted us to observe with live cell imaging how the cells were growing and dying under these conditions. We chose to use the Sartorius Incucyte to obtain these images over the course of the experiment and fine tune our experimental timeline.

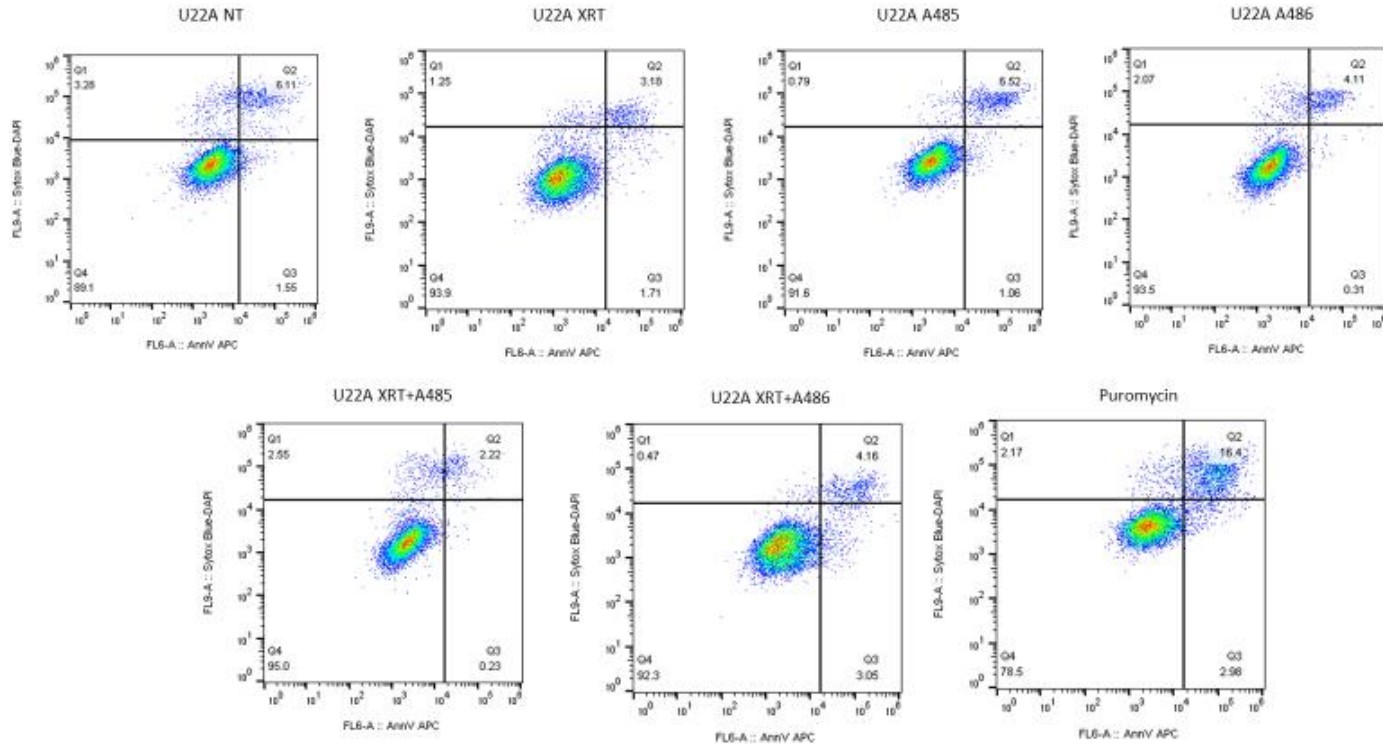


Figure 4: Flow Cytometry results analyzed through FlowJo. UMSCC22A showed no significant difference between groups treated with or without XRT, alone or in combination with HATi (A485). Quadrant I denote live cells. Quadrant II is representative of early apoptotic cells and is positive for Annexin V-APC. Quadrant III is displaying the population of cells undergoing apoptosis and is positive for Annexin V-APC and Sytox Blue. Quadrant IV represents cells at either a very late stage of apoptosis or necrosis, representing dead cells and is positive for Sytox Blue.

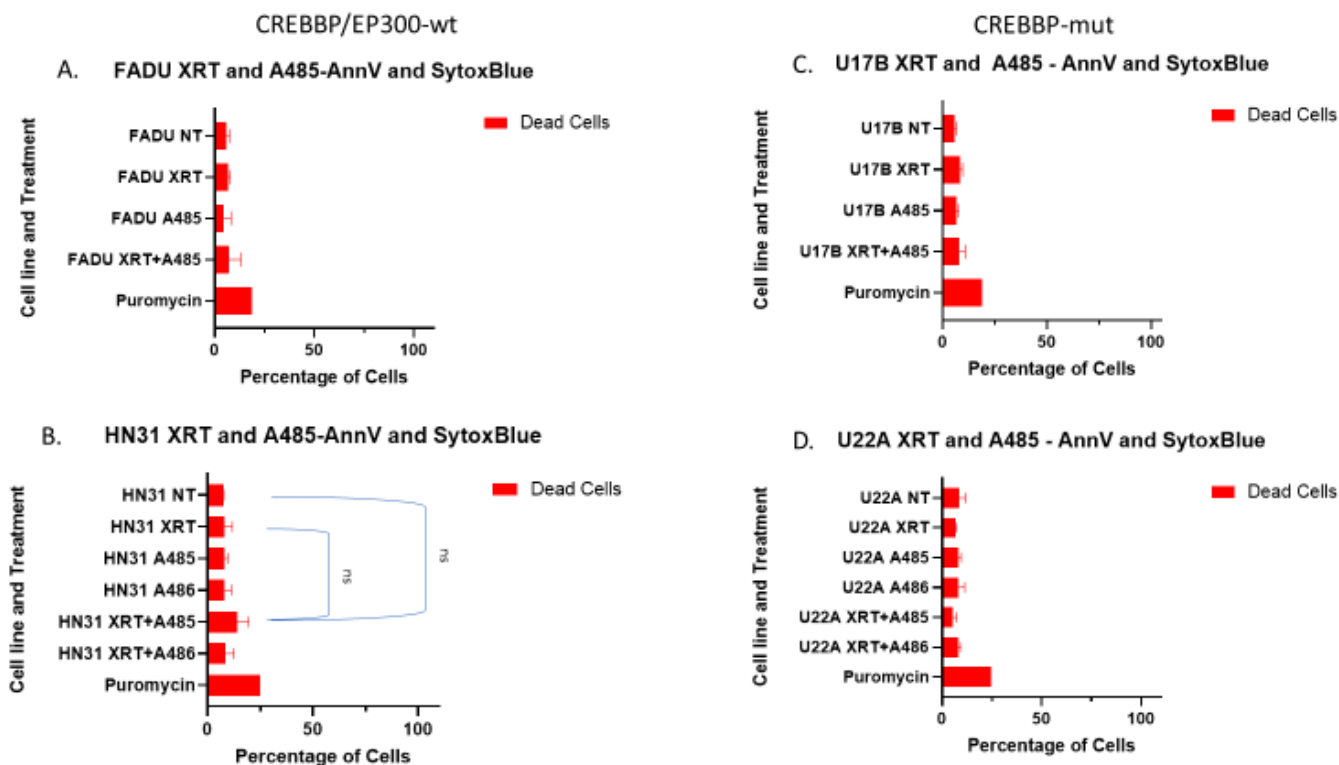


Figure 5: (A and B) CREBBP/EP300wt cell lines FADU and HN31 displayed no significant difference in the amount of cell death for conditions treated with radiation (XRT), alone and in combination with HATi (A485). (C and D) CREBBPmut cell lines UMSCC-17B and UMSCC-22A also showed no significant difference between conditions treated with XRT, alone and in combination with HAT inhibition.

No significant difference was observed between *CREBBP*mut cell lines treated with XRT or DOX and with XRT/DOX+A485

Because the previous assays performed could not confirm previous reproducible results in our labs, we decided to observe the cells growth and death with live-cell imaging via the Sartorius Incucyte. Drug dosing and plating optimization experiments were performed to find appropriate conditions for the cells in this experiment. We looked at two endpoints for these experiments: cell confluence and cell death. Figure 6 displays a normalization between the two endpoints. The cells were stained with a green Cytotox dye which is a DNA-binding dye that creates a fluorescent signal when attached to unhealthy cell's DNA. Each well's

confluence was also measured. In order to compare both measurements between each condition, we normalized these results by creating a ratio between ‘green counted objects’ and ‘phase object confluence.’ A higher value means that there was less confluence and/or more cell death. It was predicted that *CREBBP*-mut cell lines (UMSCC17B and UMSCC22A) would have significantly higher values of this ratio when treated with XRT and HATi than *CREBBP*mut cell lines treated with only one agent. A ratio was used to analyze these results because treatment with these drugs could also lead to an inhibition of growth. So, observing only cell death amongst the different treatment conditions could be misleading if, for example, the no treatment condition displayed more cell death but also had a higher confluence of cells compared to the combination condition which had equal amounts of cell death but only reached 30% confluence over the course of the experiment. As seen in Figure 6, this ratio is variable; in these findings, ‘green counted object’ can cause disrupt in the curves obtained from this experiment because of faulty images or more technical reasons. For this reason, we also looked at cell viability assays including Cell Titer Glo to confirm confluence measurements and determine how much green object count led to confusing data. HN31 cells had a significant difference between XRT only and XRT+HATi. This result is not what we predicted (Figure 6A). Figure 6B-D show no significant difference for between conditions treated with XRT alone and in combination with A-485, though it is promising that the XRT and XRT+HATi conditions curves began to separate indicating that more cell death and/or less cell growth occurs with the combination of drugs. Overall more experiments with XRT and cell health and drug dosing optimization may be needed to

observe cell growth and inhibition in the future.

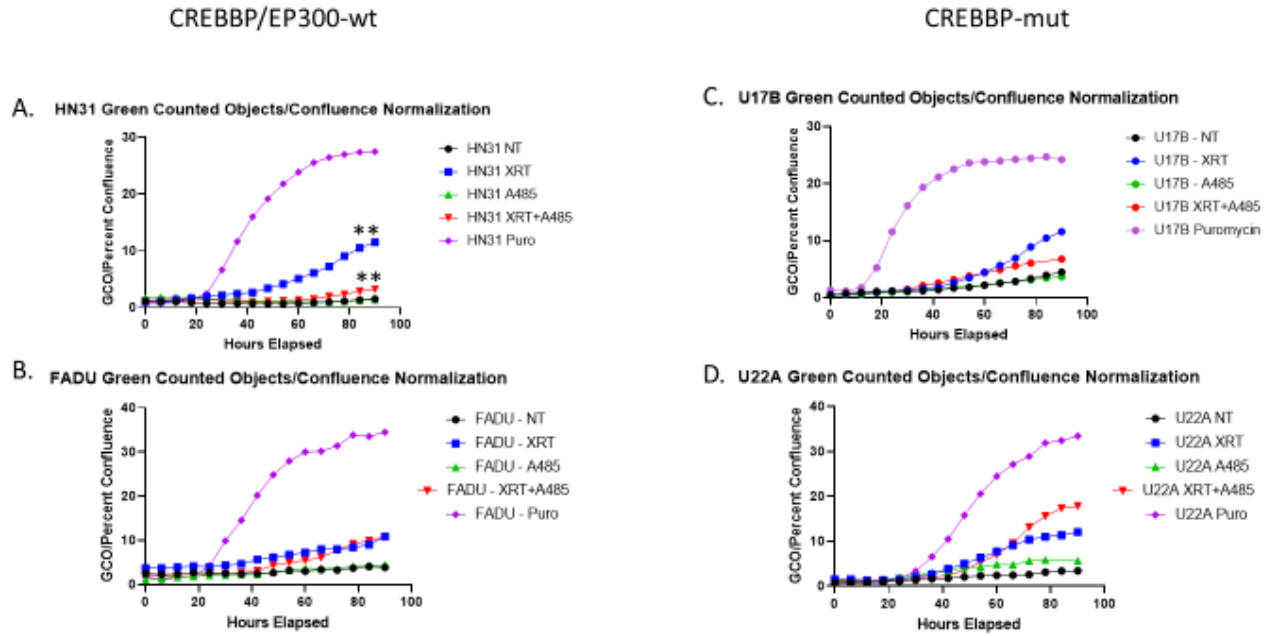


Figure 6: (A and B) display CREBBP-wt cell lines HN31 and FADU. FADU has no significant difference between conditions treated with radiotherapy alone and in combination HAT inhibition (A485). HN31 showed a significant difference between XRT and XRT+HATi conditions.

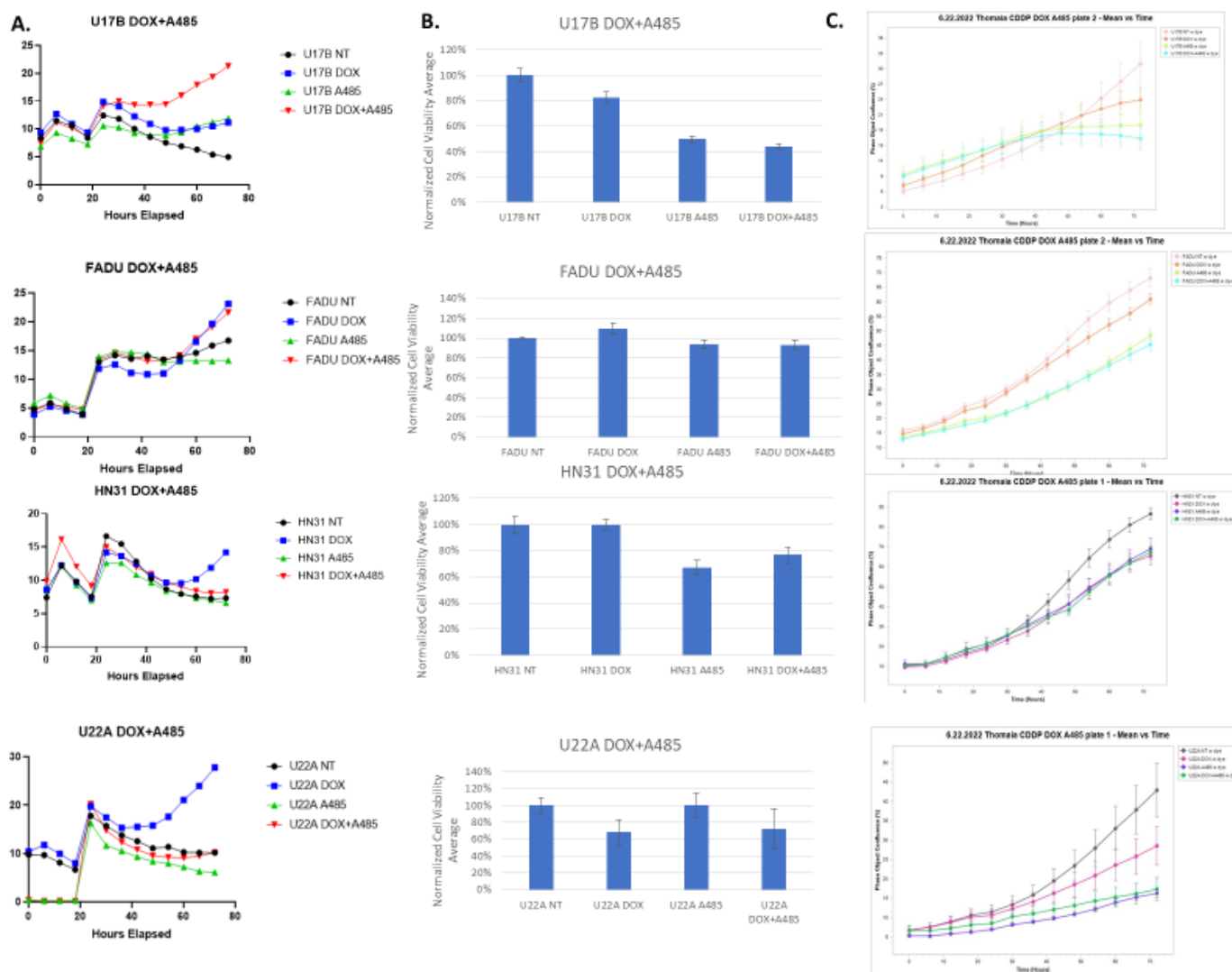


Figure 7: HNSCC cell lines with varying mutation status in CREBBP were treated with DOX alone or in combination with HAT1 (A485) and observed for three days in the Incucyte. 6A shows the results of this experiment as a ratio of green counted objects over phase object confluence. A higher value of this ratio could mean more cell death and less cell growth is occurring. 6B displays Cell Titer Glo results of the same experiments to as another measure of cell death and to compare the changes in cell death with the normalized ratio generated from the incucyte. 6C displays the confluence measurements of these cells only. From this we determined that the green counted objects measurement can create much variance when normalizing to confluence.

Apoptosis is not confirmed in CREBBPmut or WT HNSCC treated with CDDP, DOX, XRT alone or in combination with A485

The timeline for the Western blot experiment included plating cells on Day 1, treating with A485 on Day 2, treating with CDDP, DOX, or XRT on Day 3, and collecting the protein

samples on Day 4. Proteins samples were collected and then probed to identify caspase 3 and PARP proteins and cleavage products (Figure 8).

Western Blot Timeline

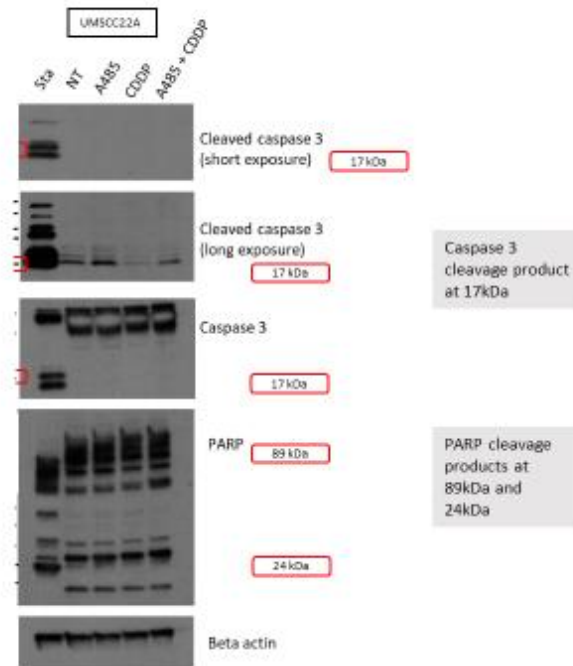


Figure 8: Treatment plan for the Western blot experiments included a 24-hour pretreatment of A485 and 24-hour treatment of CDDP, DOX, or XRT.

To investigate the type of cell death and observe a potential enhancement or reduction of a cell death response, we performed Western Blot analyses. We observed apoptotic proteins caspase 3 and poly (ADP-ribose) polymerase (PARP) which, when apoptosis is active, full length proteins are cleaved into smaller products that are sized at 17kD for caspase 3 and 89kD and 24kDa for PARP. This method would determine if my hypothesis that *CREBBP*mut HNSCC cells undergo apoptosis when combined with XRT/DOX combined with A485. Figure 9A shows UMSCC22A had neither of these specific cleavage products when the cells were treated with CDDP and A485, the HAT inhibitor. Figure 9B shows that HN31 (*CREBBP*-WT) had no specific cleavage products for caspase 3 or PARP when treated with XRT alone or in combination. However, UMSCC22A (*CREBBP*-mut) showed one faint

band at both cleavage sites for PARP and none for caspase 3. This does not definitively mean apoptosis is occurring in these conditions because cleavage products are not seen at 89kDa for PARP or in the caspase 3 Western blot.

A. UMSCC22A (mut) Cisplatin + HATi (A485)



B. HN31 (WT) and UMSCC22A (mut) Radiation + HATi (A485)

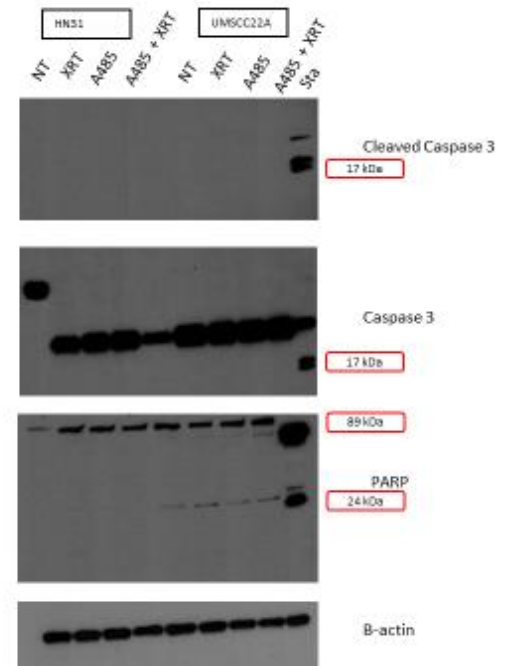


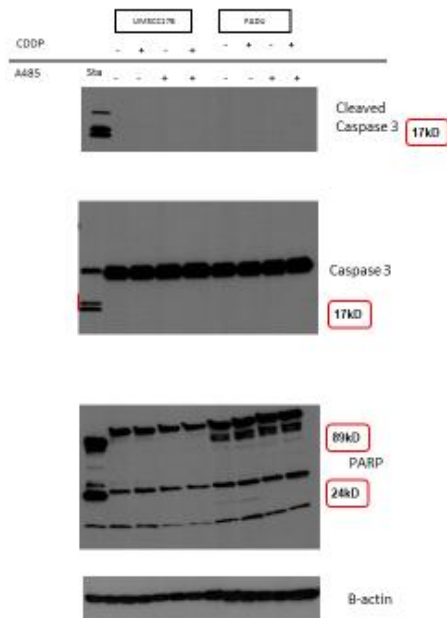
Figure 9: (A) A Western blot of UMSCC22A showed no cleavage products of apoptotic markers: caspase 3 and PARP when these cells were treated with Cisplatin (CDDP) alone or in combination with HAT inhibiting drug, A485. A longer exposure of caspase 3 did show some cleavage products, but this result was not consistent in UMSCC22A. (B) HN31 cells showed no consistent cleavage products of apoptosis markers PARP and caspase 3 when treated with radiation (XRT) alone or in combination A485. UMSCC22A did not have cleave products for caspase 3 but did show faint cleavage in the HATi + XRT condition and in other conditions.

We tested another two HNSCC cell lines: FADU (*CREBBP*-WT) and UMSCC17B

(*CREBBP*-mut). UMSCC17B showed no specific cleavage markers for caspase 3 when cells were treated with CDDP alone or in combination with HAT inhibition (A485) but did show one cleavage product in PARP (Figure 10A). FADU cells did not show cleavage products for caspase 3 but did have cleavage products for PARP. These bands did not display an

enhancement or reduction amongst different conditions however (Figure 10A). When treated with XRT, alone or in combination with A485, UMSCC17B did not have any specific cleavage products for caspase 3 or PARP. FADU cells also did not display cleavage products for caspase 3 when treated with XRT alone or in combination with A485. But with PARP, FADU had a cleavage product at 89kD for each condition and varying products shown at 24kD. Therefore, I did not observe apoptosis occurring in UMSCC17B, nor did I apoptosis occur in terms cleaved caspase 3 for FADU. FADU did show cleavage products for PARP which suggests apoptosis may be occurring in the cells, so the results are inconclusive since I do not have both PARP and caspase 3 cleavage for FADU. Also, I was determining if there was an enhancement of cell death with a combination treatment of XRT and A485, and the FADU bands shown seems to all have the same amount of product in each condition.

**A. FADU (WT) and UMSCC17B (mut)
Cisplatin + A485**



**B. FADU (WT) and UMSCC17B (mut)
Radiation + A485**

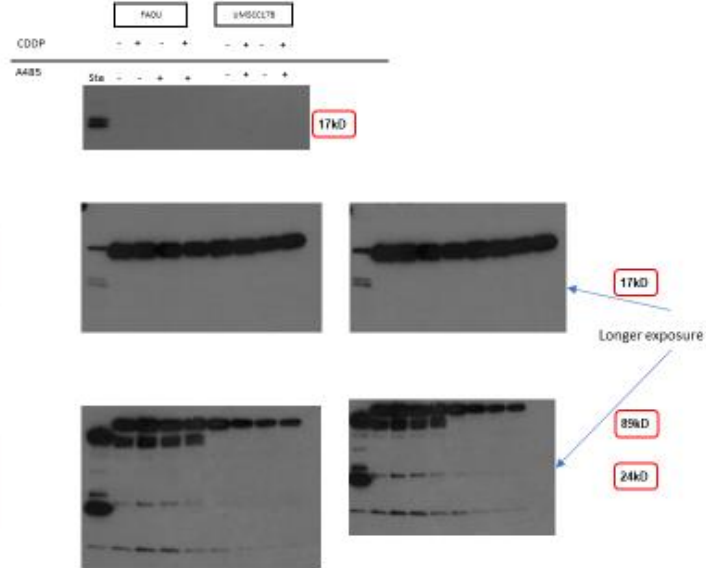


Figure 10: (A) UMSCC17B cells showed no specific cleavage products of apoptotic markers: PARP and caspase 3. FADU showed specific but similar bands across each condition, thus not showing a specific response to CDDP alone or in combination with A485. (B) UMSCC17B showed no bands at the cleavage points for PARP (89kD and 24kD) or caspase 3 (17kD). FADU (CREBBP-WT) showed cleavage products for PARP, but not caspase 3. The PARP cleavage products are nonspecific.

The lack of caspase 3 cleavage was not the same to results seen similarly by our groups in previous reproducible experiments, so to make conditions as similar as possible to when the same experiments were done in the lab previously and led to positive results, we changed the media we were using and the specific cleaved caspase 3 antibody.²⁴ With these changes, Figure 11 displays that FADU treated with XRT still did not express cleaved caspase 3 or consistent varying expression levels with PARP. UMSCC17B did not express caspase 3 but had slight expression of PARP cleavage products at 89kD and 24kD. Overall, from these Western blot assays, consistent expressions of apoptotic were not seen in most cell lines. FADU did have consistent PARP cleavage, the expressions were generally all at the same level, however.

FADU (WT) and UMSCC17B (mut) radiation + HATi

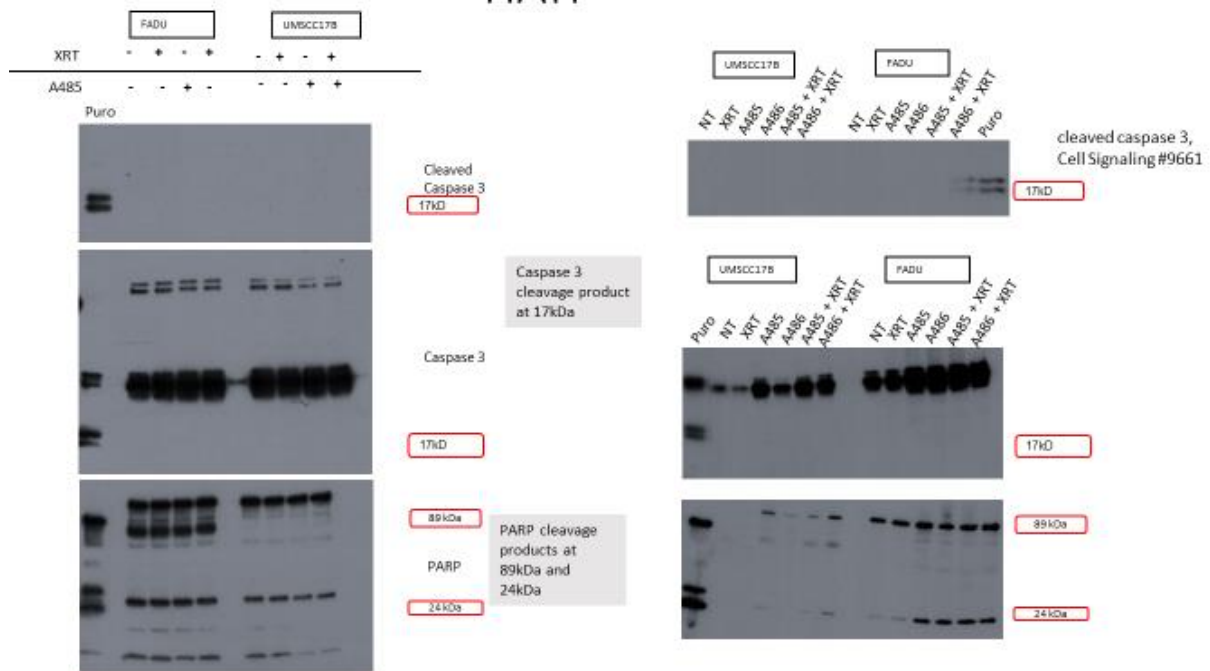


Figure 11: FADU (CREBBP-WT) and UMSCC17B (CREBBP-mut) do not show cleavage products for caspase 3, an apoptotic marker. FADU generally shows PARP cleavage products at similar levels so a difference in response to radiotherapy alone or in combination with A485 is not observed. UMSCC17B showed inconsistent bands at one cleavage point for PARP in this figure.

The positive controls in these experiments, puromycin or starosporin-treated cells, showed that some technical aspects of the assay worked. Though there could be further technical issues with the experiments that have not been discovered that prevented us from not recapitulating the past results of cleaved caspase 3 cleavage in radiation and heightened levels in the radiation and A485 combination. The project's overall results (Table 1) did not validate the hypothesis because an enhancement of cell death in XRT+HATi conditions, nor in DOX+HATi was repeatedly observed. There was also no significant difference between CDDP and DOX conditions as predicted. These experiments did not replicate the previous findings in our labs. The problem could be due to as a yet undiscovered technical problem.

Alternatively, the cells we use could have mutated over time; potentially becoming more resistant treatments or less healthy in general.

Table 1: Overview of results from each experiment. CSA is Clonogenic Survival Assay, FLOW is flow cytometry, WB is Western blot. "Neg" is negative and it means that no significant difference was seen between any of the treatment conditions. "Pos" means positive and a significant difference was seen between some of the treatment conditions. In the "pos" results, we did see a combination effect.

Cell Lines	CREBBP status	CSA	Result	Cell Lines	CREBBP status	CSA	Result	
HN31	WT	CDDP+A485	neg	HN31	WT	XRT+A485	neg	
FADU	WT	CDDP+A485	neg	FADU	WT	XRT+A485	pos	significant difference at 6Gy
UMSCC22A	mut	CDDP+A485	neg	UMSCC22A	mut	XRT+A485	neg	
UMSCC17B	mut	CDDP+A485	neg	UMSCC17B	mut	XRT+A485	pos	significant difference at 6Gy
Cell Lines	CREBBP status	FLOW	Result					
HN31	WT	XRT+A485	neg					
FADU	WT	XRT+A485	neg					
UMSCC22A	mut	XRT+A485	neg					
UMSCC17B	mut	XRT+A485	neg					
Cell Lines	CREBBP status	Incucyte	Result	Cell Lines	CREBBP status	Incucyte	Result	
HN31	WT	DOX+A485	neg	HN31	WT	XRT+A485	pos	significant difference between XRT and XRT+A485 conditions
FADU	WT	DOX+A485	neg	FADU	WT	XRT+A485	neg	
UMSCC22A	mut	DOX+A485	neg	UMSCC22A	mut	XRT+A485	neg	
UMSCC17B	mut	DOX+A485	neg	UMSCC17B	mut	XRT+A485	neg	
Cell Lines	CREBBP status	WB	Result	Cell Lines	CREBBP status	WB	Result	
HN31	WT	XRT+A485	neg	FADU	WT	CDDP+A485	inconclusive	
FADU	WT	XRT+A485	inconclusive	UMSCC22A	mut	CDDP+A485	inconclusive	
UMSCC22A	mut	XRT+A485	inconclusive	UMSCC17B	mut	CDDP+A485	inconclusive	
UMSCC17B	mut	XRT+A485	inconclusive					

Chapter 4: Discussion

Initially, our labs set out to find radiosensitization targets in HNSCC. This eventually led to the remarkable finding like that the CREBBP/EP300 KD leads to radiosensitization in HNSCC. Additionally, inhibition of CREBBP/EP300's HAT domain leads to radiosensitization and is associated with homologous repair repression. Our labs found that some mutations in CREBBP lead to a gain of function response resulting in increased protein acetylation which mediates the response to radiation.

In this project, we compared the effect of CDDP to doxorubicin because both impair different DNA damage repair pathways. CDDP impairs NHEJ while DOX impairs HR. As expected, we did not observe an increase in cell death with the combination of CDDP and HATi with *CREBBP*-mut cell lines UMSCC22A and UMSCC17B as compared to the single agents. For the XRT clonogenic assays, we observed a significant difference between in FADU (*CREBBP*wt) and UMSCC17B at the 6Gy with and without HATi. We predicted and saw in previous studies that UMSCC17B would show an increase in cell death between XRT alone and XRT in combination HATi.²⁴ However, we also saw an increase in the *CREBBP*wt, FADU cell line which was not the customarily observed result in previous studies or what we may have predicted. One reason this may have occurred is because it is the end range of the XRT dosage. The higher concentration of XRT may have sensitized the cells to A485 more. This trend was not observed in previous studies where at each dose of XRT the *CREBBP*mut cell line treated with A485 was found to be statistically significant to the condition only treated with XRT. Further clonogenic experiments must be continued to observe this trend. However, clonogenic experiments in our hands began to malfunction.

Multiple tests were done using different incubators, plates, and media, but consistent colony growth was not attainable.

To observe a potential enhancement or reduction a cell death response, we performed Western blot analyses. Caspase 3 is activated in mammals and is part of a cascade of events that leads to apoptosis. Caspase 3 stimulates chromatin condensation, DNA fragmentation, or membrane blebbing and can activate other proteins or caspases.³⁵ Poly (ADP-ribose) polymerases (PARPs) are an enzyme family that activates the transfer of ADP-ribose to their designated proteins. Some isoforms such as PARP1 and PARP2 are known for their involvement in DNA repair, studies have also shown that PARPs play an important part in cell death and proliferation.³⁶ For example, PARP has been found to activate apoptosis-inducing factor (AIF) which stimulates caspase-independent cell death.³⁷ In this study, we use caspase 3 and PARP antibodies to observe the possibility of apoptosis occurring in the cell death response we've previously observed in our lab.

In figure 9A, there are faint bands in the negative control, A485 only, and A485 combined with CDDP conditions for UMSCC22A (*CREBBP*mut), and minimal expression in the CDDP alone condition. Figure 9B displays faint bands indicating PARP cleavage in UMSCC22A (*CREBBP*mut) in the negative control group and in conditions with XRT alone or in combination with A485. Because caspase 3 and PARP specific cleavage products at 17kD and 89 and 24kD, respectively, were not observed consistently throughout the conditions in figure 4, we cannot confirm that apoptosis occurred. Cleaved caspase 3 bands expressed in the longer exposed film is also not validated by cleavage product expression with the other antibodies in the same experiment. Similar results were seen in Figure 10 where FADU showed 89kD cleavage product of PARP in all conditions when treated with

XRT and/or CDDP alone or in combination with A485, but an enhancement or reduction of this protein expression was not observed. This does suggest that apoptosis is occurring in these cells but there is not a distinction between single vs. combined treatment groups.

To observe cell death through another assay while simultaneously addressing our aim to determine if apoptosis is the method of cell death occurring in the cytotoxic response, we performed flow cytometry experiments. We were not able to validate our labs' previous results which included caspase 3 cleavage with XRT alone and in combination with A485. We adjusted our experiments by changing the media and supplements to DMEM F-12 and using only 1% Penicillin and Streptomycin, and 10% FBS. We also changed the cleaved caspase 3 antibody to match the manufacturer of the antibody used in our labs' previous findings.²⁴ Because multiple flow cytometry, clonogenic assays, and Western blotting experiments were not working in our hands, we chose to use the Incucyte to observe cell growth with live cell imaging and determine if we needed to change the timing of our treatments or collection.

Our Incucyte experiments began with optimization assays to determine what dye, initial cell density, drug dosages, and time period should be used to measure cell death with this technique. Figure 7 displays results from treating *CREBBP*wt and *CREBBP*mut cells with XRT and HATi. Though there was a distinct separation between the XRT and XRT+A485 curves, there was no statistical difference between the two conditions. We measured a statistical difference in HN31 (*CREBBP*wt) cells, however, this was not a finding consistent with previous findings from the lab. Because my hypothesis is mostly concerned with the effects of DOX the potential different phenotype from CDDP and XRT was mostly used as a control for DOX conditions, we decided for the rest of the Incucyte experiments to

focus mostly on DOX and CDDP in combination A485. In the DOX and CDDP we still did not see a significant difference between single agent and combined agent conditions.

The study's limitations included some logistical points: the COVID-19 pandemic placed a 6-month pause on research and made business travel unavailable. The latter could have been helpful in troubleshooting since the team who performed most of the experiments we were attempting to reproduce was in a distant location, more senior research scientists moved on to different opportunities so there was less support in trouble shooting was needed.

Further biological limitations could include the cell lines we were using, though we did obtain UMSCC-22A cells from Dr. Heath Skinner's lab group in Pittsburgh, PA, further investigation into the cells genotype may explain the resistance to treatment we observed. Additionally, more CREBBPmut and WT HNSCC cell lines could have been used to determine if we could get a phenotype from the agents employed in this study other cells.

Conclusion:

In conclusion, I did not see an enhancement of cell death with DOX or XRT in combination with A485 when compared to XRT or DOX as single agent in HNSCC cell lines. Beyond an enhancement of cell death, I also did not observe a reproducible and significant cell death response using only the single agents in the HNSCC cells. For future work on these studies, I would suggest further optimization to first reproduce the results found in previous studies in our lab. Then, repeating these experiments to at least obtained cell death or apoptotic phenotype in the single treated XRT condition. With more time and assistance, I believe we would see more of a response to these agents than I have outlined above.

Beyond CREBBP/EP300, there are other studies using a wide range of genomics to find radio sensitizing targets in HNSCC. One group used multiple omics data to determine a 12-gene signature to stratify patients who had higher radiosensitivity and could benefit from radiotherapy.³⁸ Another study used clonogenic survival assays to find a radiation sensitivity signature in HPV- HNSCC patients to predict the recurrence of cancer after radiotherapy. They found the recurrence-free survival rate to be significantly lower in HNSCC cell lines that were radioresistant.³⁹ Identifying predictive signatures, radio sensitizing targets, or HNSCC with specific mutation status that leads to increased radiosensitivity helps establish more personalized therapies. The head and neck region is a defining part of the human anatomy, issues here could lead to trouble speaking, eating, and breathing. It's imperative to discover fewer toxic therapies to help make the quality of life for patients better.

Patients with HNSCC have poor outcomes relatively. Much of patient death is attributed to local treatment failure. Thus, our groups' discovery that *CREBBP/EP300* knockdown led to significant radiosensitization is a step in the direction towards more targetable therapies and better patient outcomes. The labs' previous finding that A485 results in radiosensitization suggests that it or other drugs that may successfully inhibit the HAT functions in *CREBBP/EP300*mut HNSCC is novel and therapeutically relevant agents for induced cytotoxicity.

This project aimed to test the ability for doxorubicin (DOX) to show similar induced cytotoxic effect as radiotherapy (XRT) when combined with A485. We chose to look at doxorubicin because it has a similar DNA damage repair effects as XRT where cells are triggered to repair their DNA damage with homologous recombination repair. XRT and chemotherapy come with a multitude of toxic side effects such as myelosuppression and

mucositis. Determining if DOX and XRT both led to an increased cell death response would lead to further implication on how to trigger cell death and potentially decreasing the amount of XRT or chemotherapeutics needed to use on patients.

References:

1. Merck Reports Double-Digit Earnings-Per-Share Growth for Second Quarter 2007.October 12, 2007.
2. The American Cancer Society medical and editorial content team. *About Oral Cavity and Oropharyngeal Cancer What Are Oral Cavity and Oropharyngeal Cancers?* American Cancer Society. Cancer.org
3. Parsons JT, Mendenhall WM, Stringer SP, Admur RJ, Hinerman RW, Willaret DB, Moore-Higgs GJ, Greene BD, Speer TW, Cassisi NJ, Million RR. Squamous cell carcinoma of the oropharynx: Surgery, radiation therapy, or both. *Cancer*. 2002;94(11):2967-2980. doi:10.1002/cncr.10567
4. The American Cancer Society medical and editorial content team. *About Laryngeal and Hypopharyngeal Cancer*. American Cancer Society. Cancer.org.
5. Calkins H, Sousa J, El-Atassi R, Rosenheck S, de Buitleir M, Kou W H, Kadish A H, Langber J J, Morady F. Diagnosis and Cure of the Wolff–Parkinson–White Syndrome or Paroxysmal Supraventricular Tachycardias during a Single Electrophysiologic Test. *New England Journal of Medicine*. 1991;324(23):1612-1618. doi:10.1056/NEJM199106063242302
6. Kimple RJ, Smith MA, Blitzer GC, Torres AD, Martin JA, Yang RZ, Peet CR, Lorenz LD, Nickel KP, Klingehutz AJ, Lambert PF, Harari PM. Enhanced Radiation Sensitivity in HPV-Positive Head and Neck Cancer. *Cancer Research*. 2013;73(15):4791-4800. doi: 10.1158/0008-5472.CAN-13-0587

7. Galmiche A, Saidak Z, Bouaoud J, Mirghani H, Page C, Dakpe S, Clatot F. Genomics and precision surgery for head and neck squamous cell carcinoma. *Cancer Letters*. 2020; 481:45-54. doi: 10.1016/j.canlet.2020.04.004
8. Stambuk HE. Perineural tumor spread involving the central skull base region. *Seminars in Ultrasound, CT and MRI*. 2013;34(5):445-458. doi: 10.1053/j.sult.2013.09.002
9. Maxwell JH, Ferris RL, Gooding W, Cunningham D, Mehta V, Kim S, Myers EN, Johnson J, Chiosea S. Extracapsular spread in head and neck carcinoma: Impact of site and human papillomavirus status. *Cancer*. 2013;119(18):3302-3308. doi:10.1002/cncr.28169
10. Greenberg JS, Fowler R, Gomez J, Mo V, Roberts D, El Naggar AK, Myers JN. Extent of extracapsular spread. *Cancer*. 2003;97(6):1464-1470. doi:10.1002/cncr.11202
11. Bonner J, Harari P, Giralt J, Azarnia N, Shin DM, Cohen RB, Jones CU, Sur R, Kies MS, Baselga J, Youssoufian H, Amellal N, Rowinsky E, Kian Ang K. Radiotherapy plus Cetuximab for Squamous-Cell Carcinoma of the Head and Neck. *The New England Journal of Medicine*. 2006; 354:567-578. Doi: 10.1056/NEJMoa053422
12. Huang J, Zhang J, Shi C, Liu L, Wei Y. Survival, recurrence and toxicity of HNSCC in comparison of a radiotherapy combination with cisplatin versus cetuximab: a meta-analysis. *BMC Cancer*. 2016;16(1):689. doi:10.1186/s12885-016-2706-2
13. Siddik ZH. *Mechanisms of Action of Cancer Chemotherapeutic Agents: DNA-Interactive Alkylating Agents and Antitumour Platinum-Based Drugs*.

14. Sears CR, Turchi JJ. Complex Cisplatin-Double Strand Break (DSB) Lesions Directly Impair Cellular Non-Homologous End-Joining (NHEJ) Independent of Downstream Damage Response (DDR) Pathways. *Journal of Biological Chemistry*. 2012;287(29):24263-24272. doi:10.1074/jbc.M112.344911
15. Loehrer PJ, Einhorn LH. *DIAGNOSIS AND TREATMENT Drugs Five Years Later Cisplatin*. <https://annals.org>
16. Szturz P, Wouters K, Kiyota N, Tahara M, Prabhas K, Noronha V, Adelstein D, Van Gestel D, Vermorken JB. Low-Dose vs. High-Dose Cisplatin: Lessons Learned From 59 Chemoradiotherapy Trials in Head and Neck Cancer. *Frontiers in Oncology*. 2019;9. doi:10.3389/fonc.2019.00086
17. Tacar O, Sriamornsak P, Dass CR. Doxorubicin: an update on anticancer molecular action, toxicity and novel drug delivery systems. *Journal of Pharmacy and Pharmacology*. 2012;65(2):157-170. doi:10.1111/j.2042-7158.2012.01567.x
18. Carvalho C, Santos RX, Cardoso S, Correia S, Oliveira PJ, Santos MS, Moreira PI. *Doxorubicin: The Good, the Bad and the Ugly Effect*. Vol 16.; 2009.
19. Maede Y, Shimizu H, Fukushima T, Kogame T, Nakamura T, Miki T, Takeda S, Pommier Y, Murai J. Differential and Common DNA Repair Pathways for Topoisomerase I- and II-Targeted Drugs in a Genetic DT40 Repair Cell Screen Panel. *Molecular Cancer Therapeutics*. 2014;13(1):214-220. doi: 10.1158/1535-7163.MCT-13-0551

20. Codony VL, Tavassoli M. Hypoxia-induced therapy resistance: Available hypoxia-targeting strategies and current advances in head and neck cancer. *Translational Oncology*. 2021;14(3):101017. doi: 10.1016/j.tranon.2021.101017
21. Wang H huan, Fu Z guang, Li W, Li Y, Zhao L, Wen L, Zhang J, Wen N. The synthesis and application of nano doxorubicin-indocyanine green matrix metalloproteinase-responsive hydrogel in chemophototherapy for head and neck squamous cell carcinoma. *International Journal of Nanomedicine*. 2019; Volume 14:623-638. doi:10.2147/IJN.S191069
22. Moore JK, Haber JE. *Cell Cycle and Genetic Requirements of Two Pathways of Nonhomologous End-Joining Repair of Double-Strand Breaks in Saccharomyces Cerevisiae*. Vol 16.; 1996.
23. Chang HHY, Pannunzio NR, Adachi N, Lieber MR. Non-homologous DNA end joining and alternative pathways to double-strand break repair. *Nature Reviews Molecular Cell Biology*. 2017;18(8):495-506. doi:10.1038/nrm.2017.48
24. Li X, Heyer WD. Homologous recombination in DNA repair and DNA damage tolerance. *Cell Research*. 2008;18(1):99-113. doi:10.1038/cr.2008.1
25. Kumar M, Molkentine D, Molkentine J, Bridges K, Xie T, Yang L, Hefner A, Gao M., Bahri R, Dhawan A, Frederick MJ, Seth S, Abdelhakiem M, Beadle BM, Johnson F, Wang J, Shen L, Heffernan T, Sheth A, Ferris RL, Myers JN, Pickering CR, Skinner HD. Inhibition of histone acetyltransferase function radiosensitizes *CREBBP/EP300* mutants via repression of homologous recombination, potentially targeting a gain of function. *Nature Communications*. 2021;12(1). doi:10.1038/s41467-021-26570-8

26. de Guzman RN, Liu HY, Martinez-Yamout M, Dyson HJ, Wright PE. Solution structure of the TAZ2 (CH3) domain of the transcriptional adaptor protein CBP. *Journal of Molecular Biology*. 2000;303(2):243-253. doi:10.1006/jmbi.2000.4141
27. Chargi, N., Molenaar-Kujisten L, Huiskamp LFJ, Devriese LA, de Bree R, Huitema ADR., The association of cisplatin pharmacokinetics and skeletal muscle mass in patients with head and neck cancer: The prospective PLATISMA study. *Eur J Cancer*, 2022. 160: p. 92-99.
28. Wang F, Marshall CB, Ikura M. Transcriptional/epigenetic regulator CBP/p300 in tumorigenesis: structural and functional versatility in target recognition. *Cellular and Molecular Life Sciences*. 2013;70(21):3989-4008. doi:10.1007/s00018-012-1254-4
29. Shiama N. The p300/CBP family: integrating signals with transcription factors and chromatin. *Trends in Cell Biology*. 1997;7(6):230-236. doi:10.1016/S0962-8924(97)01048-9
30. Vo N, Goodman RH. CREB-binding Protein and p300 in Transcriptional Regulation. *Journal of Biological Chemistry*. 2001;276(17):13505-13508. doi:10.1074/jbc.R000025200
31. Waddell AR, Huang H, Liao D. CBP/p300: Critical Co-Activators for Nuclear Steroid Hormone Receptors and Emerging Therapeutic Targets in Prostate and Breast Cancers. *Cancers (Basel)*. 2021;13(12):2872. doi:10.3390/cancers13122872
32. Jin Q, Yu LR, Wang L, Zhang Z, Kasper LH, Lee J, Wang C, Brindle PK, Dent SYR, Ge K. Distinct roles of GCN5/PCAF-mediated H3K9ac and CBP/p300-mediated

- H3K18/27ac in nuclear receptor transactivation. *The EMBO Journal*. 2011;30(2):249-262. doi:10.1038/emboj.2010.318
33. Ogiwara H, Ui A, Otsuka A, Satoh H, Yokomi I, Nakajima S, Yasui A, Yokota J, Kohno T. Histone acetylation by CBP and p300 at double-strand break sites facilitates SWI/SNF chromatin remodeling and the recruitment of non-homologous end joining factors. *Oncogene*. 2011;30(18):2135-2146. doi:10.1038/onc.2010.592
 34. Ogiwara H, Kohno T. CBP and p300 Histone Acetyltransferases Contribute to Homologous Recombination by Transcriptionally Activating the BRCA1 and RAD51 Genes. *PLoS ONE*. 2012;7(12):e52810. doi: 10.1371/journal.pone.0052810
 35. Porter AG, Ja RU, Nicke È. *Emerging Roles of Caspase-3 in Apoptosis*. <http://www.stockton-press.co.uk/cdd>
 36. Morales J, Li L, Fattah FJ, Dong Y, Bey EA, Patel M, Gao J, Boothman DA. Review of poly (ADP-ribose) polymerase (PARP) mechanisms of action and rationale for targeting in cancer and other diseases. *Crit Rev Eukaryote Gene Expr*. 2014;24(1):15-28. doi:10.1615/critreveukaryotgeneexpr.2013006875
 37. Kondo K, Obitsu S, Ohta S, Matsunami K, Otsuka H, Teshima R. Poly(ADP-ribose) Polymerase (PARP)-1-independent Apoptosis-inducing Factor (AIF) Release and Cell Death Are Induced by Eleostearic Acid and Blocked by α -Tocopherol and MEK Inhibition. *Journal of Biological Chemistry*. 2010;285(17):13079-13091. doi:10.1074/jbc.M109.044206

38. Liu J, Mengmen H, Zhenyu Y, Dong C, Wen Pengbo W, Zhao G, Wu L, Xia J, Bin Y. Prediction of Radiosensitivity in Head and Neck Squamous Cell Carcinoma Based on Multiple Omics Data. *Frontiers in Genetics*. 2020. Doi:10.3389/fgene/2020.00960
39. Kim S, Kang JW, Noh JK, Jun HR, Lee YC, Lee JW, Kong M, Eun Y. Gene signature for prediction of radiosensitivity in human papillomavirus-negative head and neck squamous cell carcinoma. *Radiation Oncology Journal*. 2020;38(2)99-108. Doi: 10.3857/roj.101000136

VITA

Thomaia J. Pamplin is the daughter of Cora and John Pamplin. After obtaining her high school diploma from Phillips Academy in Andover, MA in 2014, she enrolled in the University of Houston (UH) in Texas. She attended UH for three semesters and finished her undergraduate work at the University of Texas at Austin where she received the degree of Bachelor of Arts with a major in English Literature in December 2018. She enrolled at the UT MD Anderson Cancer Center (MDACC) UTHealth Graduate School of Biomedical Sciences in August 2019 and in February 2020 began as a graduate research assistant at MDACC Department of Head and Neck Surgery.